2008 American Control Conference
Westin Seattle Hotel, Seattle, Washington, USA
June 11-13, 2008

Numerical studies on the hemodynamics in the human vein and venous valve

N.S. Wijeratne, K.A. Hoo*
Department of Chemical Engineering,Texas Tech University, Lubbock,TX 79409-3121

Abstract— **Proper blood flow in the veins are important to ensure effective return of deoxygenated blood to the heart. A major element of the human venous system is the presence of one-way, flexible, bicuspid valves in the legs that allow antegrade blood flow while preventing retrograde flow. Veins are elastic in nature thus their lumens can collapse under external forces and distend under internal pressures. Fluid flow within such flexible structures is regulated by the stresses imposed upon and by the structure, the material properties of the fluid, and the presence and function of the internal valve. As a result of viscous forces and fluid pressure the flexible structures are subject to continuous displacement. The primary objective of this study is to develop a two-dimensional computational model of non-Newtonian fluid flow within and around flexible structures. Accurate numerical solutions of this system provide a means of connecting venous valve incompetence and fluid flow behavior to the onset of cardiovascular limitations.**

I. INTRODUCTION

The veins in human legs contain one-way, flexible, bicuspid valves whose role is to aid in antegrade blood flow and prevent retrograde flow [1]. The venous valves consist of a pair of flexible leaflets, attached at a point to the vein wall while their free edges protrude into the vein's lumen (see Figure (1)). The venous valves in the lower extremities of the human legs divide the vein lumen into short segments and assist in relieving the vein wall from gravitational effects [2] (see Figure (2)). Furthermore, veins are more flexible when compared to arteries allowing their lumen to collapse under external forces and to distend under internal pressures. The experimental fluid flow studies of Raju et al. [3] and

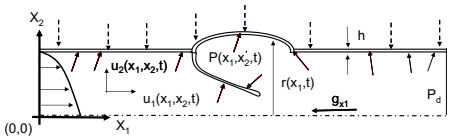

Fig. 1. Schematic of the lateral cross section of the system

also by Buescher et al. [4] show that the valve geometry, material properties of the vein and venous valve and the fluid affect the fluid dynamics of antegrade flow. In vivo studies on healthy subjects by Lurie et al. [5] suggest that there are four phases in a single valve cycle: open, closing, closed and a self excited oscillation phase at the leaflet tip. Lurie et al. also observe that fluid flow in the distal side of the vein is pulsatile and vortices may form behind the valve cusps due to flow separation at the valve edges; flow will re-attach at the sinus

*author to whom all correspondence should be sent karlene.hoo@ttu.edu

Fig. 2. Human vein and valve. Left: Mold Right: Cadaver segment.

wall. Numerical studies on a mono-leaflet heart valve by Reif et al. [6] postulate that vortex shedding at the valve edge will play a role in the flutter-like behavior in the leaflet (i.e. self excited oscillation). Therefore hemodynamics events such as flow separation, flow re-attachment and vortex formation in the valve sinus play a significant role in the valve motion thus regulating the antegrade blood flow. These implications motivate the current study to connect the mechanics and material properties of flexible structures (both venous vein and valve) with fluid properties (non-Newtonian behavior) to uncover limiting conditions.

In this study, a structure that consists of a collapsible tube with internal flexible leaflets is constructed as a surrogate for a human vein and valve. A two-dimensional mathematical representation is developed that describes the time-dependent behavior of the vein and valve system by considering two domains, specifically, the fluid domain in which the dynamics of the fluid is defined and the solid domain in which the dynamics of the flexible structures (i.e. vein and the valve) is defined. The model assumes a non-Newtonian laminar fluid flow at isothermal conditions. The fluid domain is modeled using momentum and mass conservation principles [7] and non-Newtonian material properties. The induced stresses on the flexible structures and the boundary displacements are related by Newton's second law [8]. It then follows that the mathematical description of this system involves multi-dimensional fluid dynamics and nonlinear solid mechanics resulting in a system of nonlinear partial differential equations with non-stationary boundary conditions. Initial numerical studies on collapsible tube flow by [9], [10] show that there can be significant distortions in the tube wall that deforms the fluid domain. As a result, a computational mesh in the fluid domain also deforms accordingly. To address these issues, an Arbitrary Lagrangian-Eulerian (*ALE*)

description is used to define the governing equations in the fluid domain [11]. The governing equations in the solid domain are in Lagrangian frame. Then a finite element numerical analysis method is employed to find a solution to the ALE mathematical model [12].

The organization of the paper is as follows. In section II the definition of the problem and a mathematical description of the problem are presented. The results and analysis are presented in section III. Finally section IV presents a summary of important contribution of this study. The reader also is referred to [13] for a more in depth discussion.

II. Model of the fluid and structure interaction

For the purposes of developing a mathematical formulation, a two-dimensional schematic of half of the cross section (see Figure 1) of the lateral cross section of the vein and the valve system is considered. The following assumptions are made: i) The fluid is non-Newtonian and laminar. ii) Isothermal conditions. iii) The elastic properties of the flexible structures follow a linear stress-strain relationship.

TABLE I
VARIABLE DEFINITIONS.

L,Length of the tube (m)	x_1, Axial coordinate (m)
x_2, Radial coordinate (m)	t, Time (s)
$r(x_1,t)$, Radius of the tube (m)	$u_1(\cdot,\cdot)$, Axial fluid velocity,(m/s)
$u_2(\cdot,\cdot)$, Radial fluid velocity (m/s)	$p(x\cdot,\cdot)$, Fluid pressure (Pa)
ρ, Fluid density (Kg/m^3)	μ, Dynamic fluid viscosity (Pa-s)
U_{max}, Inlet max axial vel (m/s)	P_d, Exit fluid pressure (Pa)
U, Axial displacement (m)	V, Radial displacement m)
$F_{b_{x_i}}$ Fluid forces (Pa)	μ_o, Fluid dynamic viscosity (Pa/s)
$\dot{\gamma}$, Fluid shear rate (s^{-1})	c, Spatial convective vel (m/s)
ε_{x_i}, Material strain	ε_{x_i}, Material shear strain
σ_{x_i}, Material stress (Pa)	$\tau_{x_1x_2}$, Material shear stress (Pa)
ρ_t, Vein density (Kg/m^3)	ρ_s-Valve density (Kg/m^3)
h, Tube thickness (m)	E_t, Young's Modulus-vein (Pa)
E_s,Young's Modulus-valve (Pa)	F_{x_i}, Body forces (Pa)
δ_{max}, Max tube displacement (m)	T,Temperature (C$^\circ$)
η, Temperature coefficient (1/C$^\circ$)	μ_f, Plasma viscosity (Pa/s)
C, % Hematocrit	$\dot{\gamma}_c$, critical shear rate (s^{-1})
μ_{37},Plasma viscosity at 37°C (Pa/s)	T_c, Cycle duration (s)
g_{x_i}, Gravitational force (Pa)	T, Body temp.

A. Model of the fluid domain

Fluid dynamics in a vein with an internal leaflet can be described by conservation of momentum and the conservation of mass in the *ALE* framework,

$$\frac{\partial u_i}{\partial t} + c\nabla u_j = -\frac{1}{\rho}\frac{\partial p}{\partial x_i} + g_{x_i} + \frac{1}{\rho}\nabla^2\mu u_i \quad i,j = 1,2, \quad (1)$$

$$\rho\nabla u_i = 0 \quad (2)$$

$$\text{i=1,2} \quad t > 0, \quad 0 < x_1 < L, \quad 0 < x_2 < r(x_1,t)$$

. where $c = u_i - \hat{v}$ and $\{u_i, \hat{v}\}$ are the material velocity (for a fixed material point) and mesh velocity (for a fixed mesh point) in the spatial coordinates, respectively. This model considers an upright position (i.e. standing position). Therefore, the model accounts for static pressures due to the fluid column in addition to dynamic pressures. The left hand side of the Eq. (1) accounts for acceleration and the convective acceleration of the velocity components. The pressure, gravitational, and viscosity effects are represented by the first three terms on the right hand side of this equation, respectively.

The initial and boundary conditions for Eq. (1) are as follows. A fully developed velocity condition at the entrance is assumed. Since the human vein contains a series of valves that segment the vessel, sequential opening and closing of these valves results in a periodic inflow of fluid into the vein segment. Therefore, the velocity component in the x_1 direction, $u_1(0,x_2,t)$, is assumed to follow a parabolic pattern at periodic conditions,

$$U_m = \begin{cases} U_{max}\sin\left(\dfrac{2\pi t}{T_c}\right) & (n-1)T_c \le t \le 0.5(2n-1)T_c, \\ 0 & 0.5(2n-1)T_c \le t \le nT_c \end{cases} \quad (3)$$

$n = 1,2,...$ and T_c is the duration of valve opening to valve closure. The entrance velocity component in (x_2 direction) $u_2(0,x_2,t)$-direction is assumed to be zero for all time. At $x_1 = L$, and $0 \le x_2 \le r(x_1,t)$), a fixed pressure condition P_d is prescribed that is slightly higher than the normal central venous pressure. Symmetric boundary conditions are defined at the center line, $\partial u_i(x_1,0,t)/\partial x_j = 0$, $i,j = 1,2$. At the tube wall, $0 \le x_1 \le L$ and $x_2 = r(x_1,t)$, the fluid velocity components coincide with the tube wall movement rate at respective directions i.e. $u_1(x_1,r(x_1,t),t) = \partial U/\partial t$ and $u_2(x_1,r(x_1,t),t) = \partial V/\partial t$. The initial velocity components within the tube are assumed to be zero, $u_i(x_1,x_2,0) = 0$, $0 < x_1 < L$, $0 < x_2 < r(x_1,0)$.

B. Viscosity model for blood

In this study the fluid is blood. An appropriate viscosity model is one where blood viscosity depends on the percent of red blood cell present in the fluid and plasma viscosity, and shear rate [14]. Note that the plasma viscosity is a function of the body's temperature, which is assumed to be a constant in this study. Quemada [15] provides a constitutive equation for blood viscosity using the principles of minimum energy dissipation,

$$\begin{aligned} &\mu = \mu_f\left(1 - \frac{k}{2}C\right)^{-2} \qquad k = \frac{k_o + k_\infty(\dot{\gamma}/\dot{\gamma}_c)^{0.5}}{1 + (\dot{\gamma}/\dot{\gamma}_c)^{0.5}} \\ &k_o = \exp(3.874 - 10.41C + 13.8C^2 - 6.738C^3) \\ &k_\infty = \exp(1.3435 - 2.803C + 2.711C^2 - 0.6479C^3) \\ &\dot{\gamma}_c = \exp(-6.1508 + 27.923C - 25.6C^2 + 3.697C^3) \end{aligned} \quad (4)$$

where the parameters k_o, k_∞ and $\dot{\gamma}_c$ are functions of the % hematocrit present in blood. An equation for plasma viscosity (μ_f) is given by [16],

$$\mu_f = \mu_{37}\exp\left[\eta(37 - T)\right] \quad (5)$$

C. Model of the solid domain

The solid domain consists of a collapsible tube with an embedded valve where each domain has different material properties. As a result of the combined effects of fluid

pressure, viscous forces, and external forces, the stresses induced on the boundaries result in structural deformation. The induced stresses (i.e. normal and shear stresses) on the structures are related to the strains in the respective directions via the elastic modulus. The strains are estimated by calculating the relative displacements of a infinitesimal continuum. The stress-strain relationship and the displacement are given by,

$$\varepsilon_{x_1} = \frac{\partial U}{\partial x_1}, \varepsilon_{x_2} = \frac{\partial V}{\partial x_2}, \varepsilon_{x_1x_2} = \frac{1}{2}\left(\frac{\partial U}{\partial x_2} + \frac{\partial V}{\partial x_1}\right)$$
$$\sigma_{x_1} = E_t\varepsilon_{x_1}, \sigma_{x_2} = E_t\varepsilon_{x_2}, \tau_{x_1x_2} = E_t\varepsilon_{x_1x_2}$$

.

1) Equations of motions for flexible tube wall: The motion of the flexible structures can be described by the conservation of momentum. The induced stresses can be expressed as functions of the relative displacements and Young's modulus using the relationship described in the preceding section. Thus, by considering the forces acting on an infinitesimal continuum of the tube, the relationship between induced stresses, body forces, and the displacements of the continuum in Lagrangian framework are given by,

$$\frac{\rho_t d^2U}{dt^2} = E_t\left[\nabla^2 U + \frac{\partial^2 V}{\partial x_1 \partial x_2}\right] + F_{x_1} \tag{6}$$

$$\frac{\rho_t d^2V}{dt^2} = E_t\left[\nabla^2 V + \frac{\partial^2 U}{\partial x_1 \partial x_2}\right] + F_{x_2} \tag{7}$$

for $t > 0, 0 < x_1 < L, r(x_1,t) < x_2 < h + r(x_1,t)$. The terms on the left hand side of the above equations represent the rate of change in the momentum of the infinitesimal continuum in their respective directions. The terms on the right hand side represent the induced normal and shear stresses and the body force acting on the continuum. The forces acting on the internal boundaries of the tube and also on the leaflet boundaries consist of the fluid pressure and the viscous forces,

$$F_{b_{x_i}} = A_{x_i}(-p_{x_i} + (\nabla(\mu\bar{U}))_{x_i} + (\nabla(\mu\bar{U}))'_{x_i} \quad i = 1,2 \tag{8}$$

where $\bar{U} = [u_1 \quad u_2]'$ is the velocity vector.

The initial and boundary conditions are as follows. The edges at the end of the tube wall ($x_1 = 0, L$, $r(x_1,t) \leq x_2 \leq h + r(x_1,t)$) are assumed to be fixed in space in both directions, that is, $U(0,x_2,t) = 0, U(L,x_2,t) = 0, V(0,x_2,t) = 0$, and $V(L,x_2,t) = 0$. The inner boundary of the tube wall ($x_2 = r(x_1,t)\,\forall x_1$) is subjected to pressure and viscous forces exerted by the fluid. $F_{b_{x_i}}, i = 1,2$. Periodic muscle contraction and expansion exert periodic compressive forces and displacements on the outer vein wall. Additionally, due to asymmetric geometry of the muscle, the extent of the force or the displacement exerted on the outer vein wall segment may be nonuniform every where along the vein segment. To represent these dynamics, the outer boundary of the tube wall ($x_2 = h + r(x_1,t)\,\forall x_1$) is subjected to a small distributed periodic displacement given by,

$$V(x_1,x_2,t) = \begin{cases} G_1 \times G_2 & (n-1)T_c \leq t \leq 0.5(2n-1)T_c, \\ 0 & 0.5(2n-1)T_c \leq t \leq nT_c \qquad n = 1,2,\ldots \end{cases}$$
$$G_1 = \delta_{max}\sin\left(\frac{2\pi t}{3}\right)$$
$$G_2 = \frac{[x_1(x_1-L)(x_1-L-0.09)(x_1-L-0.135)]}{L^4} \tag{9}$$

Initially there is no stress or displacement acting on the any of the boundaries of the tube leading to zero initial displacements defined by $U(x_1,x_2,0) = 0$, and $V(x_1,x_2,0) = 0, \forall x_1,x_2$.

2) Equation of motion for the flexible valves: The axial and the radial motions of the leaflet can be represented by set of partial differential equations similar to Eqs (6) and (7), with boundary conditions given by the sum of viscous and pressure forces acting on the all boundaries ($F_{b_{x_i}}, i = 1,2$) of the valve that may come in contact with the fluid. The valve boundary that is attached to the tube wall is considered spatially fixed for all time. The initial displacements of all the boundaries are assumed to be zero.

D. Mathematical integration of the fluid and solid interactions

With the governing Eqs (1) and (2) in the fluid domain, the spatial fluid properties can be computed at each time step by implementing a finite element method. Then, the current pressure and viscous forces that acts on the flexible boundaries are used as inputs to Eqs (6) and (7) to estimate the movement of the boundaries. Also, the finite element method is used to calculate the nodal displacements within the flexible structure. Due to the movement of the boundaries, the mesh points in the fluid domain also are displaced. Thus, before calculating the fluid properties at the nodal points at the next time step, the mesh positions must be updated. Once the boundary motions are known for the current time step, the internal mesh node movements are calculated from $\nabla(\hat{v}) = 0$. This procedure is repeated for the entire time span.

In this work, fluid velocities and solid domain displacements are represented by quadratic shape functions while fluid pressure is represented using linear shape functions. For numerically accurate and convergent results, it is important to guarantee that the computational mesh is less distorted for all time. When moving objects are present in the computational domain, the Comsol support services [17] recommend using a sectioned domain followed by meshing the individual sections such that the number of nodal points are matched along the sectional boundaries. This technique allows controlling the individual mesh deformation. In this model, the number of nodal points along the sectional and external boundaries are prescribed to control the number of mesh elements in each section. This has resulted in both triangular and quadrilateral mesh elements. Table II lists the mesh statistics and the computational parameters used for convergence.

III. Results

The governing equations for the fluid structure interactions given in the previous sections are solved by employing finite element method. Femlab®Multiphysics software (Comsol) v 3.3a is used to carry out the numerical simulations. The parameter valves are given in Table III.

A. Fluid flow dynamics in the collapsible tube with one-way valve

Figure 3 shows the axial velocity profile when the valve is open. The approximate centerline axial velocity distally, between the leaflets, and proximally are about 7 cm/s, 17 cm/s, and 13 cm/s, respectively. These values are in the in the range provided by [5] measurements. Further analysis indicate (not shown here) that the fluid flow Reynolds numbers are in the range of 5 to 25. The motion of the valve leaflet changes from 0.35 cm/s to 0.72 cm/s and at the open position the free edge of the valve leaflet is about 0.35 cm (See second panel of Figure 5) from the center line.

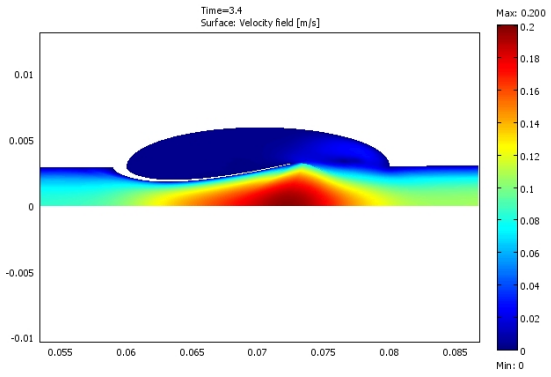

Fig. 3. Axial fluid velocity at valve open position.

Figure 4 shows the streamline patterns during a single cycle of closing and opening of a vein segment in an upright position. This analysis is carried out by with hematocrit percent of 30%. Referring to the simulation it has been estimated that a single cycle duration is about 3.0 seconds. The closed phase occurs at 0.2 second and the opening phase is about 0.3 second. The equilibrium phase is about 1.5 seconds and closing phase is about 1 second. The durations for the valve cycle, opening phase and equilibrium phase are in good satisfactory agreement when compared to the *in vivo* results of [5]. However, the closing phase and closed phases are different when compared to their estimates. These variations may be attributed to to the parameter valves used in the simulation as well as the frequency of the external compression. In spite of these timing differences, the model is able to capture the fluid dynamics of the vein valve system confirming the formation of vortices that modulated the valve motion.

Also it has been observed that there is deformation in the tube during the entire simulation. However, deformation in the tube is much less compared to the displacement of the leaflet. (Note due to the scaling of the figures deformation in the tube may not be visible.) Formation of a vortex during the valve opening phase can be seen from the second to fourth panels of Fig. 4. During the equilibrium phase vortex shedding is observed and this can be postulated to the existence of self-excited oscillations.

B. Vortex shedding due to flow separation at the leaflet

Figure 5 shows the variation in the fluid shear rate at the leaflet free edge and the right panel shows the movement of the leaflet free edge. These unsteady shear rates are indicative of self-excited oscillations. Referring to the motion of the leaflet edge it can be deduced that there is a small frequency oscillation. However, the simulation results for the leaflet edge motion does not show high frequency oscillations.

C. Stress analysis on the leaflet free edge

As the fluid flows from distal to proximal, the free edge of the leaflet moves vertically performing the valve opening and closure mechanisms. During the valve opening phase there are flow separation and vortex formation; and during the equilibrium phase, there is vortex shedding at the leaflet's free edge. These events induce normal and shear stresses on the free edge and ultimately cause motion of the leaflet's free edge (see bottom panel of Figure 6).

Figures 7 and 8 show the normal stresses acting in the radial and axial directions and surface shear stress acting on the free edge of the leaflet. All these stresses exhibit periodic behaviors.

D. Sensitivity analysis due to % hematocrit

Figure 9 shows the effects of changing the percent hematocrit in the blood in the viscosity model on valve opening. It has been estimated that with 30% hematocrit present the valve open position is about 0.355 cm from the center line and with an increase in percent hematocrit to 50% the valve open position ceases at 0.3 cm. As expected an increase in percent hematocrit increases the viscosity of the blood creating higher viscous forces inside the sinus that affects the movement of the leaflet.

IV. Summary

In this study the authors present a two-dimensional model to represent flow dynamics around the human vein and venous valve found in the legs of humans. The mode was developed using fundamental principals of fluid structure interactions. Simulation result enabled an estimation of the extent of the valve opening and also visualization of structures such as vortex formation and their role in flow regulation and valve motion. A sensitivity analysis at different hematocrit values showed the impact of blood thinning or thickening on the overall motion of the valve. The model is able to predict reasonable flow dynamics that may take place in the actual vein and valve system. Therefore, this type of model can provide useful insights to medical community when treating serious diseases such as chronic venous insufficiency.

REFERENCES

[1] P.S. Bemmelen, G. Bedford, K. Beach, and D. E. Strandness. Quantitative segmental evaluation of venous valver reflux with duplex ultrasound scanning. *J. Vascular Surgery*, 10(4):425–431, October 1989.

[2] F. E. Hossler and R. F. West. Venous valve anatomy and morphometry: Studies on the duckling using vascular corrosion casting. *The American Journal of Anatomy*, 181:425–432, 1988.

[3] S. Raju, C. A. Hudson, R. Fredericks, P. Neglen, A.B. Greene, and E.F. Meydrech. Studies in calf venous pump function utilizing a two-valve experimental model. *Eur. J. Vascular and endovasclualr surgery*, 17:521–532, June 1999.

[4] C.D. Buescher, B. Nachiappan, J. Brumbaugh, K. A. Hoo, and H. F. Jansen. Experimental studies of the effects of abnormal bicuspid valves on fluid flow. *Bio Technology in Progress*, 21, 2005.

[5] F. Lurie, R. L. Kistner, B. Eklof, and D. Kessler. Mechanism of venous valve closure and role of the valve in circulation: A new concept. *J. Vascular Surgery*, 38(5):955–961, 2003.

[6] T.H. Reif and Huffstutler Jr. M.C. Design considerations for the omniscience pivoting disc cardiac valve prosthesis. *Int. J. Artif. Organs*, 6:131–138, 1983.

[7] R.B. Bird, W.E. Stewart, and E.N. Lightfoot. *Transport Phenomena*. John Willey & Sons,Inc., 2 edition, 2002.

[8] Q.S. Nguyen. *Stability and Nonlinear Solid Mechanics*. John Wiley & Sons, New York, NY, 2000.

[9] T.J. Pedley and X.Y. Luo. Modeling flow and oscillations in collapsible tubes. *Theoretical and Computational Fluid dynamics*, pages 277–294, 1998.

[10] N. S. Wijeratne and K.A. Hoo. An analytical approach to identify fluid flow separation and re-attachment in a collapsible channel. *Computers and Chemical Engineering*, 31:346–360, 2007.

[11] J. Donea, A. Huerta, J.-Ph. Ponthot, and A. Rodriguez-Ferran. *Arbitrary Lagrangian-Eulerian Methods*, volume 1 of *Encyclopedia of computational Mechanics*, chapter 14, pages 1–25. John Wiley & Sons Ltd., 2004.

[12] B.A.Finlayson. *Nonlinear Analysis in Chemical Engineering*. McGraw-Hill, 1980.

[13] N. S. Wijeratne and K.A. Hoo. Non-newtonian fluid flow model of blood flow around venous valves. *submitted to Biotechnology Progress*, Sept 2007.

[14] J.D. Zydney, A.L.and Oliver III and C.K.Colton. A constitutive equation for the viscosity of stored red cell suspensions:effect of hematocrit, shear rate, and suspending space. *Journal of Rheology*, 35(8):1639–1680, November 1991.

[15] D Quemada. Rheology of concentrated disperse systems and minimum energy dissipation principle. 1. viscosity -concentration relationship. *Rheol. Acta*, 16:82–84, 1977.

[16] S. De Grottela, K. Boomsma, and D Poulikakos. Computational simulation of a non-newtonian model of the blood separation process. *Artificial Organs*, 29(12):949–959, 2005.

[17] Solution no :970, title:improving convergence for ale and parameterized geometry. http://www.comsol.com/support/knowledgebase/970/.

[18] J.S. Ackroyd, M. Pattision, and N.L. Browse. A study of the mechanical properties of fresh and preserved human femoral vein wall and valve cusps. *Br.J. Surg.*, 72:117–119, February 1985.

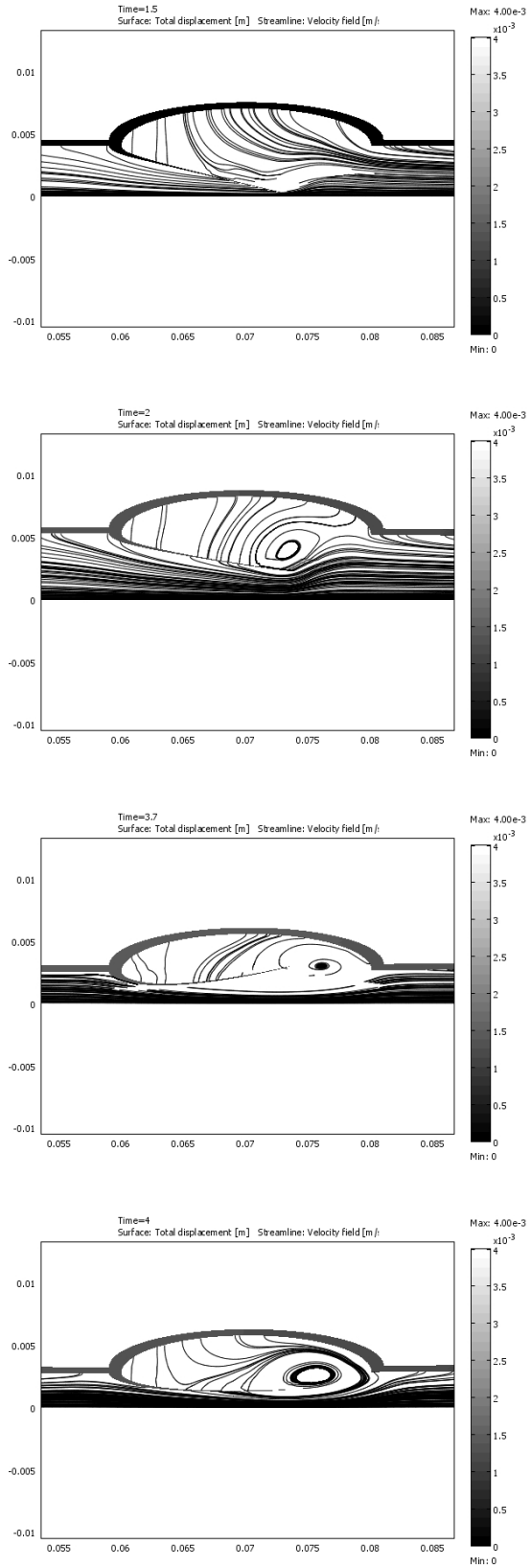

Fig. 4. Fluid streamlines at different times during a single cycle.

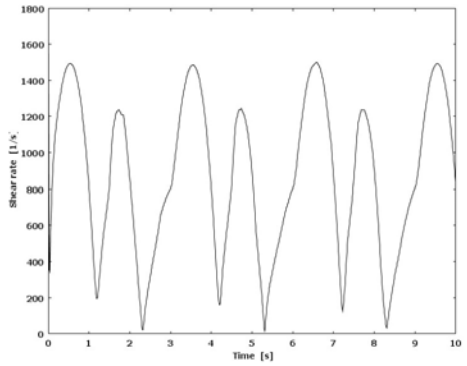

Fig. 5. Rate of change in shear rate at the leaflet's free edge.

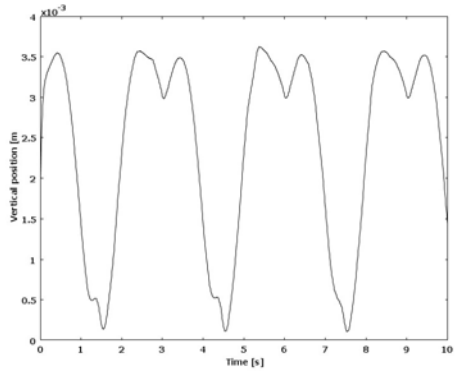

Fig. 6. Motion of the leaflet free edge.

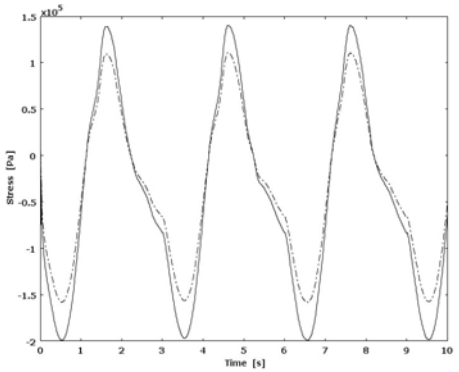

Fig. 7. Normal stress at leaflet free edge. Solid line:Stress in radial direction Dash line: Stress in axial direction.

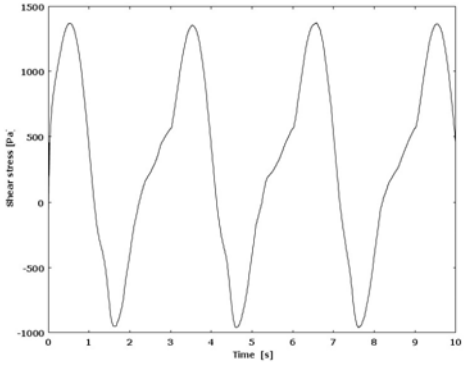

Fig. 8. Shear stress at leaflet free edge.

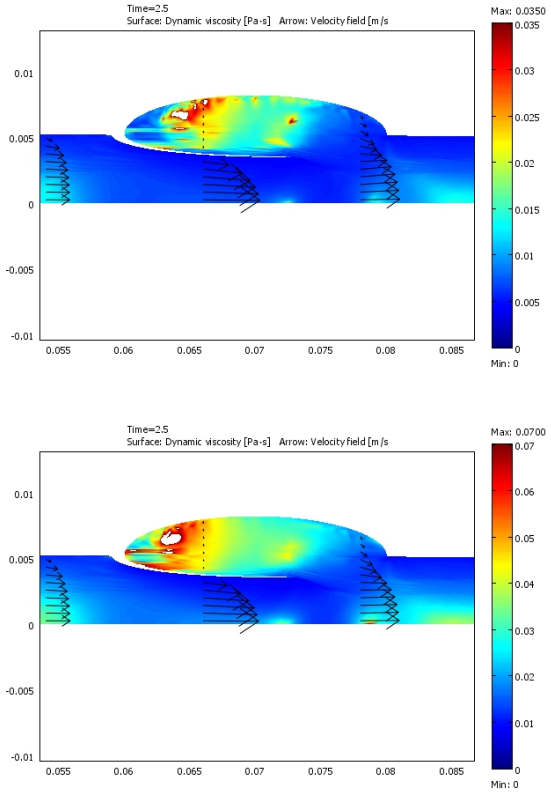

Fig. 9. Open position for different Hematocrit percentage. Top: 30% Hematocrit. Bottom: 50% Hematocrit.

TABLE II

COMPUTATIONAL PARAMETERS.

Parameter	Value
Number of mesh elements	2797
Number of triangular elements	260
Number of quadrilateral elements	2537
Solution time	8 minutes
Relative tolerance	0.001
Absolute tolerance	0.0001

TABLE III

PARAMETER VALUES[18], [16]

Symbol	Valve	Symbol	Valve
L	0.18 m	$r(0,t)$	0.004 m
C	0.3	ρ	1060 Kg/m^3
U_{max}	0.4 m/s	P_d	1000 Pa
μ_o	0.0022 Pa/s	ρ_t	960 Kg/m^3
ρ_s	500 Kg/m^3	h	0.000025 m
h	0.005 m	E_t	3.3×10^6 Pa
E_s	15×10^6 Pa	δ_{max}	0.00025 m
μ_{37}	1.4×10^{-3} Pa/s	η	0.021 $1/^\circ C$
T	28 $^\circ C$	T_c	3 s